Comparison of Convective Mass and Heat Transports in Tropical Easterly Waves Computed by Two Methods[1]

ROBERT A. HOUZE, JR., AND COLLEEN A. LEARY

Department of Atmospheric Sciences, University of Washington, Seattle 98195

(Manuscript received 28 July 1975, in revised form 21 November 1975)

ABSTRACT

Convective fluxes of mass and heat in tropical easterly waves were computed by a slightly modified version of the method of Austin and Houze (1973). The input data for this method are radar and raingage observations of cloud heights and precipitation amounts. The computed fluxes were compared to convective fluxes inferred from budget studies of synoptic-scale rawinsonde data for the same easterly waves. Good agreement between the two methods was obtained for mass and heat fluxes in the middle troposphere. For the lower troposphere, our calculations showed smaller transports of mass and heat than were indicated by large-scale budget studies. This result arises because many shallow convective clouds do not precipitate and thus are not included in calculations based on precipitation data. When the effects of small clouds (tops below 6 km) were removed from the calculations based on large-scale budgets, excellent agreement was obtained in the lower as well as middle troposphere. This study shows that a particularly useful approach in future studies will be a combination of methods based on both precipitation and large-scale data.

1. Introduction

Because of their short lifetimes and small horizontal scale, convective clouds are difficult to observe directly. Yet because of their large numbers and frequently large vertical extent, the heat, mass and moisture transports by these clouds play an important role in the dynamics of tropical disturbances and the general circulation (e.g., Riehl and Malkus, 1958; Charney and Eliassen, 1964; Palmén and Newton, 1969). The recent Global Atmospheric Research Program Atlantic Tropical Experiment (GATE) was conceived specifically to investigate the interaction between cumulus and larger scales of motion through intensive observational studies. In GATE, scales of motion from cumulus through synoptic were investigated, and now a variety of diagnostic schemes may be used to draw information on convective-synoptic scale interaction out of data sets compiled from rawinsonde, aircraft, radar and satellite observations.

Cumulus modeling techniques are used in conjunction with standard rawinsonde observations to diagnose properties of convective cloud groups from their observed effects on the large-scale environment (e.g., Yanai *et al.*, 1973; Ogura and Cho, 1973). These methods, however, do not employ observations on the scale of individual convective clouds. Austin and Houze (1973; hereafter referred to as AH), Houze (1973) and Lopez (1973) take the opposite approach. They use cumulus modeling techniques in conjunction with radar observations of the clouds themselves to deduce the properties of populations of cumulonimbus clouds.

In more specific terms, Yanai *et al.* (1973) and Ogura and Cho (1973) calculate vertical eddy flux divergences of dry static energy and water vapor, i.e., $\partial(\overline{s'\omega'})/\partial p$ and $\partial(\overline{q'\omega'})/\partial p$ (where s is the dry static energy, p is pressure, $\omega = dp/dt$, q is water vapor mixing ratio, a bar denotes an area average, and a prime denotes a deviation from the area average), as residual terms in the large-scale area-averaged equations governing the heat and moisture budgets of the atmosphere. They assume that these residuals, computed from large-scale data, are due solely to cumulus convection, and use cumulus modeling to compute the properties of the clouds responsible for the eddy fluxes.

AH and Houze (1973) use a direct product of the convection, namely its precipitation, as an indicator of convective cloud properties. They determine the amount of rain produced by convective clouds and the heights of the clouds from quantitative radar data, or from a combination of radar and raingage data, and employ a cumulus model to compute the properties of the clouds which produced the observed rain.

Convective fluxes computed from precipitation data by AH's method and from rawinsonde data using large-scale budget techniques can serve as valuable checks on each other. This paper describes such a test. We have computed convective transports of mass and heat from radar and raingage input, using a slightly modified

[1] Contribution No. 348, Department of Atmospheric Sciences, University of Washington.

version of AH's technique. The results of these calculations have been compared to cloud transports inferred by large-scale methods for the same synoptic systems (tropical easterly waves). This comparison is much more rigorous than the tests made by Houze (1973), who compared cumulus-scale fluxes computed by AH's method with fluxes due to larger scales of motions.

For the tropical wave disturbances described below, we expect the two methods to yield similar results in the middle and upper troposphere, where deep cumulonimbus clouds predominate. AH's method, however, is based on precipitation data, and the convective transports computed by this method are those due only to precipitating clouds. The large-scale method, on the other hand, includes the contribution of shallow, non-precipitating cumuli to the total flux, and should therefore show greater total mass and heat transports in the lower troposphere. The results of our study confirm these expectations.

2. Data and methods of analysis

Reed and Recker (1971; hereafter referred to as RR) composited three months of surface and rawinsonde data for a triangle of stations located in the equatorial western Pacific during the wet season (July through September) of 1967. They stratified the observations into eight categories centered on the trough axis, the ridge axis, and six intermediate positions with respect to easterly waves identified by oscillations of the vertically averaged meridional wind. When the observations were averaged within each category, they obtained the properties of a composite easterly wave, derived from the 18 wave disturbances which passed through their network during the three-month period.

In a later study, Reed and Johnson (1974) applied the method of Yanai *et al.* (1973) to RR's composite easterly wave to diagnose by large-scale methods the average properties of the cloud populations in each of the eight categories. More recently, Johnson (1975) has used Ogura and Cho's (1973) method to calculate explicitly the contributions of different cloud-size categories to the average convective fluxes in the trough of RR's composite wave. Similar computations with the RR data have been made by Cho and Ogura (1974). While some of Johnson's results are presented later in Figs. 2 and 3, a detailed account of his work is reserved for future publication.

For our comparison of AH's method with those of Reed and Johnson (1974) and Johnson (1975), we obtained radar data for Kwajalein, one of the three stations in RR's triangle. These data consist of written descriptions of the FPS-41 (10 cm wavelength) radar scope displays on the U. S. Department of Commerce, Weather Bureau, WB Form 610-3. These descriptions contain information about echo-top heights which we used in conjunction with RR's raingage analysis to compute vertical transports of mass and heat by a

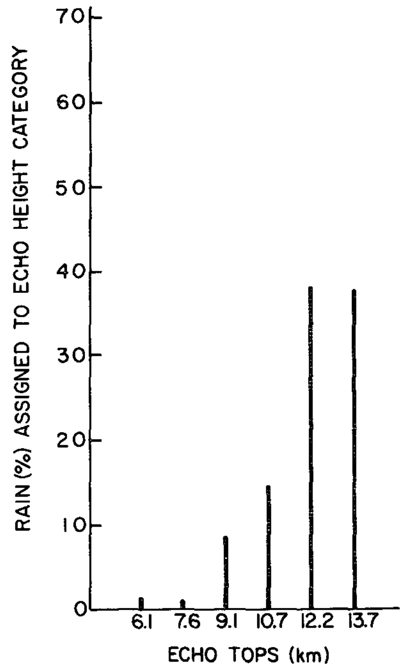

FIG. 1. Percentage of rainfall in wave-trough region found to be associated with different radar echo heights.

population spectrum of clouds of different heights in the trough region of RR's easterly waves. These computations are described in detail in Section 3.

The Kwajalein radar station reported a range of echo-top heights. We assumed that the maximum reported tops at each observation were the ultimate heights attained by the clouds which produced the observed precipitation.

The average rainfall rate in the trough region of RR's composite easterly wave was 5 mm $(6\ h)^{-1}$. The total (three-island average) rainfall for each 6 h interval during the three-month period was known from RR's analysis of raingage data. Our analysis included only those intervals attributed to the trough axis category by RR. We assigned to each of these intervals the maximum reported echo-top height as determined from the Kwajalein radar records. It was therefore possible to determine the percentage of the total wave-trough rainfall associated with each echo-height category and construct the echo-height vs rainfall spectrum shown in Fig. 1. An alternate spectrum obtained using an average rather than the maximum reported echo-top height gave physically unreasonable results when used in convective transport calculations.

3. Computation of convective transports from radar and precipitation data

a. *Mass flux*

The convective transports we computed are those required for the cloud population in the trough-axis category of RR's wave to maintain over the entire wave-trough region the observed average rainfall rate of 5 mm (6 h)$^{-1}$. Our procedure was first to compute the masses of air (M_u and M_d) displaced upward and downward in convective clouds in order to produce the amount of rainfall (5 mm) which fell over the wave-trough region in a 6 h period. No explicit time or space scales were assigned to individual clouds; however, it was assumed that the cloud updrafts and downdrafts all took place within the 6 h period of observation and at some location within the area encompassed by the large-scale trough. With this assumption it was then possible to convert M_u and M_d to convective mass *fluxes* (mass per unit area per unit time), F_u and F_d, respectively, which are representative of the wave-trough region as a whole, and can be compared with the mass fluxes deduced for the same region from large-scale observations by Reed and Johnson (1974) and Johnson (1975).

The masses of air M_u and M_d transported vertically in convective clouds are summations of contributions from clouds of the different sizes in the cloud population spectrum of Fig. 1. Thus

$$M_u = \sum_{i=1}^{6} M_{u_i}, \qquad (1)$$

$$M_d = \sum_{i=1}^{6} M_{d_i}, \qquad (2)$$

where M_{u_i} and M_{d_i} are the masses of air transported vertically to produce the observed rain which fell from clouds of size category i.

b. Cloud water budget

To compute M_{u_i} and M_{d_i} requires a water budget to infer the total amount of water condensed in convective clouds from a knowledge of observed rainfall. In the present study, we assumed that 74% of the water condensed in updrafts fell to the surface as rainfall, 13% was re-evaporated in downdrafts, and 13% was detrained to the environment or remained aloft as cloud droplets.

This precipitation efficiency (74%) is considerably greater than that found in empirical studies of continental thunderstorms in either mid-latitudes (Braham, 1952) or the tropics (Betts, 1973). There exist no empirical studies of cloud water budgets for cumulonimbus clouds over the tropical oceans; however, we expect tropical maritime clouds in RR's easterly wave to be more efficient than continental clouds because of the broader drop-size distributions and more effective particle coalescence processes associated with oceanic clouds. Moreover, cloud-cloud interactions in the cumulus ensemble may produce a higher net precipitation efficiency than can reasonably be expected for a single cumulonimbus. For example, water substance detrained from one cloud which ends up as precipitation in another contributes to the precipitation efficiency of the cumulus ensemble. Water budgets for tropical maritime cumulonimbus clouds have been obtained indirectly as a by-product of parameterization studies of cloud properties deduced from large-scale data. For cloud clusters over the tropical Pacific, Yanai *et al.* (1973) diagnosed a precipitation efficiency of 84%. Using the same method, Reed and Johnson (1974; see their Fig. 7) computed an efficiency of approximately 60% for RR's trough region, while Johnson's (1975) recent recalculation of the cloud population properties using Ogura and Cho's (1973) scheme indicated an efficiency of 77% in the trough region. Using a simpler cumulus population model, RR themselves deduced a precipitation efficiency of 75% for the clouds in the wave-trough category.

Our assumption of 74% efficiency is thus consistent with results obtained from large-scale budget studies, and we obtained the best agreement with the large-scale studies when this value was assumed. To test the sensitivity of our calculations to the efficiency assumption, we recalculated all of the convective transports assuming that 50% of the water condensed in updrafts fell to the surface as rainfall, 25% was re-evaporated in downdrafts, and 25% was detrained to the environment or remained aloft as cloud droplets. It produced convective mass and heat fluxes larger than our results shown in Figs. 2 and 3 at all levels above 1.6 km. The difference was greatest in the middle troposphere where the less efficient cloud budget produced transports greater by about a factor of 1.5 than the cloud water budget with a 74% precipitation efficiency.

c. Computations of M_{u_i} and M_{d_i}

Assuming the cloud budget described above, we obtain M_{u_i} following exactly the procedure outlined by AH to solve their Eq. (6), with M_{u_i} replacing AH's M_c. M_{u_i} was obtained for each of the six cloud-size categories included in Fig. 1 by assuming that M_{u_i} is the updraft mass transport responsible for condensing the amount of precipitation assigned to its size category in Fig. 1. To obtain M_u, the summation in Eq. (1) was carried out.

AH's study did not provide a method for computing the downdraft mass transports M_{d_i} and M_d. Since empirical studies such as those of Braham (1952), Malkus (1954) and Betts (1973) suggest that downdrafts are dynamically important, we have included an estimate of their effects in the present study. The assumptions described below allow a rough estimate of the effects of downdrafts without obscuring the computed effects of updrafts.

The analog to AH's Eq. (6) for downdrafts is

$$V_i = -\int_{z_B}^{z_{Td}} M_{d_i}\left[E(q'-q_d)-\frac{dq_d}{dz}\right]dz, \qquad (3)$$

where V_i is the mass of condensed water re-evaporated in the downdrafts of clouds of size i, z_B the height of cloud base, z_{Td} the height of the top of the downdraft, E the entrainment rate, q_d the water vapor mixing ratio in the downdraft, and q' the mixing ratio of air entrained into the downdraft. Both V_i and M_{d_i} are positive quantities in (3).

The following assumptions were made to solve Eq. (3) for M_{d_i}.

(i) In accordance with the assumed cloud water budget described above, V_i was assumed equal to 13% of the total water condensed in updrafts of clouds of size i.

(ii) The downdraft top z_{Td} was assumed to be halfway between cloud base and observed cloud top.

(iii) The profile of M_{d_i} was assumed to be linear, increasing from zero at z_{Td} to a maximum at cloud base.

(iv) The downdraft was assumed to be saturated at a temperature 1°C cooler than the synoptic-scale environment.

(v) The air entrained into the downdraft (q') was assumed to be saturated at the temperature of the synoptic-scale environment (i.e., for the purpose of computing entrainment effects, the downdraft is envisioned as being immediately surrounded by air moistened by earlier convective activity, as discussed by AH).

(vi) The entrainment rate for the downdraft was assumed to be the same as that assumed for the updraft by AH.

d. Heat flux

The convective heat flux for RR's trough region is given by

$$F_h=\sum_{i=1}^{6}\left[F_{u_i}(h_u-h_e)_i-F_{d_i}(h_d-h_e)_i\right], \quad (4)$$

where h is the moist static energy given by

$$h=C_pT+Lq+gz, \quad (5)$$

where C_p is the specific heat of dry air, T temperature, L the latent heat of vaporization of water, q water vapor mixing ratio, g gravitational acceleration, and h_u, h_d and h_e are the values of h in the updraft, downdraft and large-scale environment, respectively. Values of $(h_u-h_e)_i$ are obtained using a one-dimensional cumulus model, exactly as described by AH. Values of $(h_d-h_e)_i$ are obtained using assumption (iv) above.

4. Results

a. Mass flux

Convective mass fluxes deduced from radar and precipitation data for RR's wave-trough region are shown by the heavy solid curve in Fig. 2. The right-hand portion of the curve shows the mass flux due to updrafts only (F_u), while the left-hand portion shows the net convective mass transport (F_u-F_d). The magnitude of the mass flux due to downdrafts (F_d) is indicated by the difference between the two portions of the heavy solid curve in Fig. 2. The left-hand portion of the heavy solid curve (F_u-F_d) is the appropriate one to be compared with the net convective mass transport diagnosed by Reed and Johnson (1974) from large-scale rawinsonde data (dotted curve in Fig. 2). From this comparison it can be seen that our results agree with those of Reed and Johnson (1974) within a factor of 2 at most levels. Exceptions are found above the 14 km level, where the mass fluxes tend to zero, and in the lower troposphere where the large-scale method used by Reed and Johnson indicates fluxes of as much as a factor of 3 larger than ours.

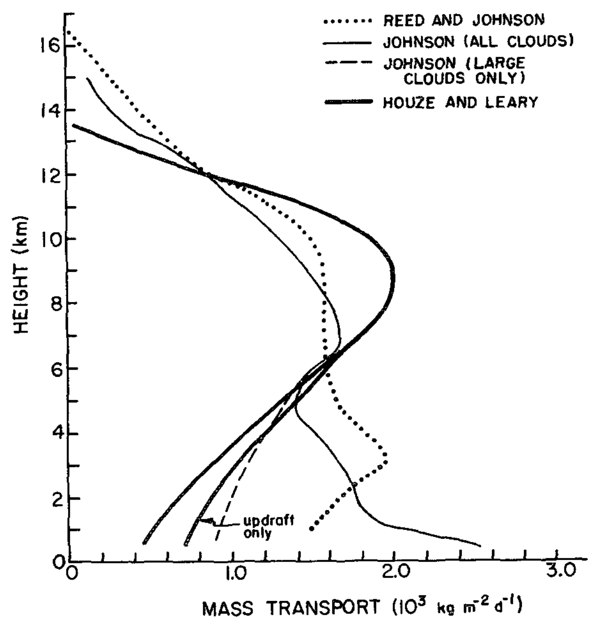

FIG. 2. Average convective mass flux in wave-trough region computed from radar and precipitation data by Houze and Leary and from large-scale data by Reed and Johnson. Further explanation in text.

As was noted in the Introduction, the larger transports in the lower troposphere obtained by Reed and Johnson (1974) are expected since their diagnostic scheme included non-precipitating cumuli which are not included in the radar-precipitation calculations. To test this interpretation further, Johnson recalculated the convective mass flux in RR's trough region using Ogura and Cho's (1973) diagnostic scheme. With this method, which is also based on large-scale observations, it is possible to compute both the convective mass transport due to all clouds (light, solid curve in Fig. 2) and that due only to clouds with tops extending above the 6 km level (dashed curve in Fig. 2). As with Reed and Johnson's calculations, Johnson's all-cloud curve exceeds our curve by a considerable amount in the lower troposphere; however, Johnson's large-cloud curve is in excellent agreement with the radar-precipitation calculations.

b. Heat flux

The convective heat flux in RR's trough-axis category computed from radar and precipitation data is shown by the heavy solid curve in Fig. 3. Heat fluxes computed from large-scale rawinsonde data by Reed and Johnson (1974) are shown for comparison with our results in the same format as Fig. 2. Reed and Johnson's and Johnson's curves should be compared with the left-hand portion of the heavy solid curve which shows the total convective heat flux F_h computed from Eq. (4). The right-hand portion of the heavy solid curve shows only the contribution of the updraft term in Eq. (4) to the total heat flux. By comparing the two portions of the heavy solid curve in Fig. 3 with each other, it can be seen that downdrafts contributed negatively to F_h. This result arose because the large-scale environment in RR's trough sector was quite dry compared with the air in the saturated convective downdrafts, and the moist static energy difference $(h_d-h_e)_i$ in (6) was dominated by the latent heat difference $L(q_d-q_e)_i$.

Comparisons between the convective heat fluxes computed by the authors from radar and precipitation data and those computed by Reed and Johnson from large-scale data may be made from Fig. 3. In the middle and upper troposphere, all of the calculations are in generally good agreement, while in the lower troposphere our results correspond most closely with Johnson's large-cloud calculation which ignores the transport due to shallow non-precipitating cumuli. A similar result was noted for the mass transports shown in Fig. 2. The difference between Johnson's all-cloud curve in Fig. 3 and the previous result of Reed and Johnson is due to the fact that in the earlier study the moisture field was truncated above the 300 mb level and in Johnson's recalculation moisture parameters were extrapolated to the 100 mb level.

Reed and Johnson's heat fluxes in Fig. 3 are somewhat larger than our values in the region between 4 and 8 km. This result is largely explained by differences in methods of computing temperature differences between updrafts and environment. Using a thermodynamic method, Reed and Johnson (1974) obtained an average updraft temperature anomaly (weighted by mass flux) of about 3°C in the 4–8 km region, while we used AH's dynamic calculation of the buoyancy required to produce a cloud of observed depth and obtained a mass-flux weighted average temperature difference of about 2°C in the 4–8 km region (see Fig. 4). Obviously, better agreement would have been obtained between the heat flux calculations shown in Fig. 3 if we had used the same temperature computing scheme as did Reed and Johnson (1974). However, we made no alteration of our calculation since there is no evidence that either temperature computing scheme gives a more accurate representation of actual clouds.

5. Conclusions

We conclude that convective transports of mass and heat can be diagnosed from either large-scale rawin-

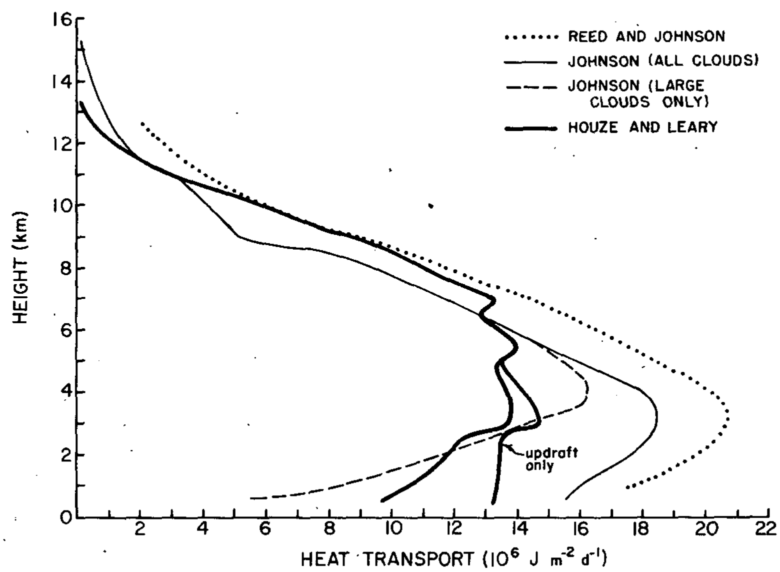

FIG. 3. Average convective heat flux in wave-trough region computed from radar and precipitation data by Houze and Leary and from large-scale data by Reed and Johnson. Further explanation in text.

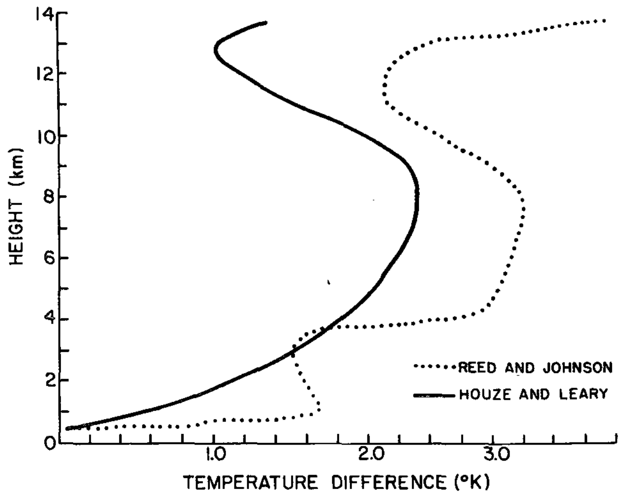

FIG. 4. Mass-flux weighted average temperature difference between cloud updrafts and large-scale environment for wave-trough region. Further explanation in text.

sonde data or small-scale radar and precipitation data, provided appropriate models are employed to interpret the data. In particular, AH's method for computing convective transports of mass and heat from radar and precipitation data gives a reliable estimate of the vertical transport due to deep cumulonimbus clouds in the disturbed trough region of tropical easterly waves.

These results indicate that a particularly useful approach in analyzing GATE data will be a combination of methods based on both small- and large-scale data. Since quantitative radar data are available over the GATE area with much greater time and space resolution than the rawinsonde data, the use of AH's method will lead to a much more detailed knowledge of the convective transports over the GATE area than could be obtained from the rawinsonde data alone.

Acknowledgments. We wish to thank Mr. Richard H. Johnson for making computations for comparison with our results and Prof. R. J. Reed for reading the manuscript and offering helpful comments. This research was supported by the Global Atmospheric Research Program, National Science Foundation, and the U. S. GATE Project Office, National Oceanic and Atmospheric Administration, Grant OCD-14830 and NSF Grant GA32439.

REFERENCES

Austin, P. M., and R. A. Houze, Jr., 1973: A technique for computing vertical transports by precipitating cumuli. *J. Atmos. Sci.*, **30**, 1100–1111.

Betts, A. K., 1973: A composite cumulonimbus budget. *J. Atmos. Sci.*, **30**, 597–610.

Braham, R. R., Jr., 1952: The water and energy budgets of the thunderstorm and their relationship to thunderstorm development. *J. Meteor.*, **9**, 227–242.

Charney, J. G., and A. Eliassen, 1964: On the growth of the hurricane depression. *J. Atmos. Sci.*, **21**, 68–75.

Cho, H.-R., and Y. Ogura, 1974: A relationship between cloud activity and the low-level convergence as observed in Reed-Recker's composite easterly waves. *J. Atmos. Sci.*, **31**, 2048–2065.

Houze, R. A., Jr., 1973: A climatological study of vertical transports by cumulus-scale convection. *J. Atmos. Sci.*, **30**, 1112–1123.

Johnson, R. H., 1975: The role of convective-scale precipitation downdrafts in cumulus-synoptic-scale interactions. Ph.D. dissertation, University of Washington, 135 pp.

Lopez, R. E., 1973: Cumulus convection and larger scale circulations: II. Cumulus and mesoscale interactions. *Mon. Wea. Rev.*, **101**, 12, 856–869.

Malkus, J. S., 1954: Some results of a trade-cumulus cloud investigation. *J. Meteor.*, **11**, 220–237.

Ogura, Y., and H.-R. Cho, 1973: Diagnostic determination of cumulus cloud populations from observed large-scale variables. *J. Atmos. Sci.*, **30**, 1276–1286.

Palmén, E., and C. W. Newton, 1969: *Atmospheric Circulation Systems*. Academic Press, 603 pp.

Reed, R. J., and E. E. Recker, 1971: Structure and properties of synoptic-scale wave disturbances in the equatorial western Pacific. *J. Atmos. Sci.*, **28**, 1117–1133.

——, and R. H. Johnson, 1974: Diagnosis of cloud population properties in tropical easterly waves. *Preprints Intern. Tropical Meteorology Meeting*, Nairobi, Kenya, Part II, Amer. Meteor. Soc., 50–55.

Riehl, H., and J. S. Malkus, 1958: On the heat balance in the equatorial trough zone. *Geophysica*, **6**, 503–538.

Yanai, M., S. Esbensen and J.-H. Chu, 1973: Determination of bulk properties of tropical cloud clusters from large-scale heat and moisture budgets. *J. Atmos. Sci.*, **30**, 611–627.